# Global microbial necromass contribution to soil organic matter

**Yuan Liu** ( liuyua14@msu.edu )
Michigan State University https://orcid.org/0000-0001-8350-5773
**Jing Tian**
China Agricultural University
**Nianpeng He**
Institute of Geographic Sciences and Natural Resources Research, Chinese Academy of Sciences
https://orcid.org/0000-0002-0458-5953
**Lisa Tiemann**
Michigan State University https://orcid.org/0000-0003-0514-6503

**Article**

**Keywords:** soil organic matter, microbial necromass, nitrogen, carbon

**Posted Date:** May 20th, 2021

**DOI:** https://doi.org/10.21203/rs.3.rs-473688/v1

# **Title:** Global microbial necromass contribution to soil organic matter

Yuan Liu[1*], Jing Tian[2*], Nianpeng He[3], Lisa K. Tiemann[1]

[1] Department of Plant, Soil and Microbial Sciences, Michigan State University, East Lansing, MI, 48823, USA.

[2] College of Resources and Environmental Sciences, National Academy of Agriculture Green Development, Key Laboratory of Plant-Soil Interactions, Ministry of Education, China Agricultural University, Beijing, 100193, China.

[3] Key Laboratory of Ecosystem Network Observation and Modeling, Institute of Geographic Sciences and Natural Resources Research, Chinese Academy of Sciences, Beijing, 100101, China.

[*] These authors contributed equally to this work.

**Soil organic matter (SOM) plays an important role in mitigating climate change and sustaining soil health and food production [1,2]. Mounting evidence suggests that microbial necromass is the main contributor to SOM [3]; however, we lack quantification of microbial necromass at a global scale, especially in subsoils. Here, we generate, for the first time, global distribution maps of microbial necromass carbon (C) and nitrogen (N) and contributions to SOM in topsoil and subsoil. Globally, necromass concentrations varied widely across ecosystems and by latitude, contributing 19-60% to SOC and 41-92% to soil N stocks, with particularly large accumulations in boreal and tropical ecosystems. On average, fungal necromass contributions to SOM are 3x greater than bacterial, although this varied across ecosystems. Microbial necromass contributions to SOC are strongly associated with soil C:N ratios and pH; necromass contributions are greater in soils with narrow C:N ratios and higher pH. Microbial necromass is on average 23 and 77 times greater than living microbial biomass in topsoil and subsoil, respectively. These data highlight the importance of necromass contributions to SOM, especially soil N, and the need for spatially resolved necromass data sets that can be used in biogeochemical models to estimate SOM dynamics more accurately.**

As the keystone of soil health and the dominant nutrient pool in terrestrial ecosystems, SOM contains more C than the atmosphere and terrestrial vegetation combined [4]. Therefore, a better understanding of the mechanisms underlying the formation and stabilization of SOM is critical for many climate change mitigation strategies and for providing the foundations for food security [1,2,5]. Traditional views suggest that selective preservation and molecular recalcitrance determine the long-term persistence of SOM [4], while emergent views suggest that SOM persistence is largely due to complex interactions between SOM, microorganisms and soil minerals [6]. Chemically, it appears that much of the C stabilized onto mineral fractions - 40-80% of SOC [3] - originates from microbial necromass, with a longer lifespan than plant derived SOM [7]. Indeed, incorporation of microbial necromass into models significantly improves model performance [8]; however, the model simulated contributions of microbial necromass to SOC (10-27%) that were much lower than previously measured [3]. Lack of explicit quantification of microbial necromass contributions to SOM at the global scale [3], especially in subsoils [9], greatly hampers our ability to constrain and incorporate soil microbial processes into biogeochemical models, which is needed to precisely predict soil responses to management, agricultural intensification and potential feedbacks to climate change [8].

Amino sugars are major components of microbial cell walls and have widely been used as biomarkers to track microbial residues [3]. Muramic acid exclusively originates from bacteria, whereas glucosamine occurs in either fungal or bacteria cell walls [10]. Fungal and bacterial necromass C and N can be estimated by measuring amino sugar biomarkers in the soil and then multiplying by conversion factors based on previously determined molecular stoichiometry of the biomarkers [3]. Using this approach, and a relatively limited data set (n=122), Liang et al. (2019) estimated that microbial necromass comprises ~30-60% to total SOC in temperate topsoil [3].

Using a comprehensive global dataset (n=902) of amino sugar concentrations in both topsoil (0-30 cm) and subsoil (30-100 cm) from peer-reviewed literature and our own data (Extended Data Fig. 1, Extended Data Fig. 2 and Supplementary Data), we demonstrate for the first time a strong and universal correlation between total soil N (TN) and amino sugars (Extended Data Fig. 3). This is important because measuring TN is relatively inexpensive and standardized, while measuring amino sugars is relatively rare, expensive, and time consuming. Therefore, researchers and modelers can now use this robust relationship to estimate

52 microbial necromass contributions to SOM across different ecosystems at a large scale without having to
53 measure amino sugars in every soil. While the relationship between TN and amino sugars has been reported
54 [11], the limited data sets in previous studies were not large enough to establish the strong universal and by
55 ecosystem type relationships we report here. We demonstrate the power of using this relationship by
56 extrapolating soil amino sugar (Extended Data Fig. 4) and then microbial necromass distributions at a global
57 scale using existing global soil TN data at a spatial resolution of 0.083° (~10 km). Global amino sugar
58 concentrations were converted to global microbial necromass C and N using previously estimated
59 stoichiometric conversion factors [11, 3].

60

61 **Global distribution of microbial necromass**

62 Concentrations of microbial necromass C varied by ecosystem and latitude with the highest
63 concentrations in boreal and tropical ecosystems (Fig. 1a, d, Extended Data Fig. 5a, b), which were estimated
64 to contain 321 and 408 Pg microbial necromass C in topsoil and subsoil, respectively (Table 1, Extended Data
65 Table 1). In tundra and boreal ecosystems microbial necromass C stocks in subsoil were much higher than in
66 topsoil (Table 1, Extended Data Table 1). At a global scale, microbial necromass C, on average, represented
67 19 to 60% of total SOC across different biomes, with similar contributions to topsoil and subsoil (Table 1,
68 Extended Data Table 1). Within different biomes, tundra had the lowest microbial necromass contribution to
69 SOC (19%, Fig. 1b, e), also reflected in its low ratio of necromass C to living microbial biomass C (MBC,
70 Table 1) compared to other biomes. This is likely a result of slow growth and turnover of microbial biomass
71 at low temperatures [12]. Apart from tundra, boreal and tropical forests also had relatively lower microbial
72 necromass contributions to SOC compared with other ecosystems (Table 1). Relatively higher lignin versus
73 protein in forest ecosystem organic matter inputs [13] or a low rhizosphere- to- bulk soil ratio in forests compared
74 with other ecosystems could decrease SOC accumulation due to relatively low C transformation rates and
75 efficiency [14].

76 We present the first ever estimates of microbial necromass N as well as its global distribution. Similar
77 to microbial necromass C, we found a high accumulation of microbial necromass N in boreal and tropical
78 ecosystems in the whole soil profile (Fig. 1g, j, Extended Data Fig. 5d, e). Globally, microbial necromass N

was estimated to contribute 49 and 63 Pg N to topsoil and subsoil N stocks, respectively (Table 1, Extended Data Table 1). We found very large microbial necromass N contributions to TN which varied from 41 to 92% across biomes, with an average of 77% globally (Table 1, Extended Data Table 1). The lowest microbial necromass N contribution to TN was found in the tundra (41.1%), and the highest in temperate forests (91%) and temperate grasslands (92%, Fig. 1h, k, Table 1). Our estimation of microbial necromass N contributions to TN are the same magnitude as a rough estimation based on microbial stoichiometry [15], which suggested that microbial sourced N can account for more than 80% of the soil TN. Amino sugar N only accounts for 0.8-13.8% of TN [16] but, other highly abundant and potentially necromass in origin N-bearing compounds (proteins, peptides, and free amino acids), overall make up as much as 78% of TN [17]. The much higher microbial necromass contributions to TN compared to SOC were potentially due to the relatively low turnover rate of microbial proteins compared to more C- rich microbial biomass constituents [18]. Based on these data, we suggest that microbial necromass is an important nutrient reservoir, and a further understanding of the decomposition and stabilization of microbially derived TN could help us to improve nutrient management in agroecosystems.

**Fungal and bacterial necromass contributions**

Across different biomes, fungal necromass was the main contributor to SOM compared with bacterial necromass (Fig. 1c, f, i, l, Table 1). At a global scale, in the whole soil profile, fungal necromass contributed 13-43%, and 31-75% to total SOC and TN pools, respectively (Extended Data Fig. 6, Extended Data Fig. 7, Extended Data Table 2). Bacteria necromass contributed 4-17%, and 10-25% to total SOC and TN pools, respectively (Extended Data Fig. 6, Extended Data Fig. 7, Extended Data Table 2). Fungal versus bacterial contributions to SOC and TN were similar in topsoil and subsoil (Extended Data Fig. 6, Extended Data Fig. 7). There are several explanations for greater fungal vs. bacterial necromass in SOM stocks. Fungi likely contribute a greater proportion of C than bacteria due to wider biomass C:N ratios and generally higher substrate use efficiencies, leading to greater fungal biomass and then necromass C produced relative to C lost as $CO_2$ [19]. Also, formation of hyphal condensed tannins and melanin complexes [20], and higher sorption rates of melanized hyphae to soil minerals [21], significantly slow fungal necromass decomposition and increase

incorporation into stable SOM.

The ratio of fungal to bacterial necromass contributions to SOM tended to increase with increasing latitude (Fig. 1). On average, the fungal to bacterial necromass ratio was lowest in tropical and subtropical forests (1.8) and was highest in temperate forests (4.7, Table 1, Extended Data Table 1), due to a relatively higher fungal necromass contribution in higher latitudes with bacterial necromass contributions being relatively constrained globally, except in the tundra (Extended Data Fig. 6, Extended Data Fig. 7). This is consistent with global living microbial biomass patterns, which show a dominance of fungal biomass with increasing absolute latitude [22] and increasing dominance of ectomycorrhizal fungi at high latitudes, which can decelerate of fungal necromass decay [23]. Lower inhibition of fungal growth at low temperatures, with bacterial growth less inhibited by higher temperatures may also drive this pattern [24].

**Drivers of necromass contributions to SOC**

At the global scale, random forest analysis showed that microbial necromass C contributions to SOC were strongly associated with soil C:N ratio and soil pH (Fig. 2a-d). The microbial necromass C contributions to SOC increase as soil C:N ratios narrow in both topsoil and subsoil (Fig. 2e, g). While the relationship is correlative, a causative relationship makes sense because a narrowing of soil C:N ratios would indicate alleviation of microbial N limitation, which would lead to increased microbial biomass production and substrate or C use efficiency (CUE) [25], and ultimately, increased microbial necromass accumulation [14] and contributions to SOC.

Soil pH was also a strong predictor of microbial necromass contributions to SOC, as pH increased microbial necromass contributions to SOC increased (Fig. 2f, h). Increases in soil pH have been shown to increase overall microbial CUE [26]. This effect is apparently more important than a concomitant shift in fungi and bacteria relative abundance. Fungi are favored by acidic conditions, and are generally considered to have a greater CUE than bacteria [27]. Therefore, we expected to see a decrease in microbial necromass C contributions to SOC accompanied by decreasing fungal biomass with increasing pH. While a bit surprising, this result supports the idea that pH is a driver of microbial community structure and CUE beyond just

132 controlling fungal to bacterial ratios [28].

133

134 **Links between necromass and living biomass**

135 Quantitative connections between living microbial biomass and microbial necromass are a rarity [15] and
136 because living microbial biomass is estimated to represent less than 4% of SOM it is often ignored in terms
137 of SOM accrual [3]. Using a recently generated global living microbial biomass dataset [29], we estimated the
138 ratios of microbial necromass to living biomass C and N at a global scale. The living microbial biomass does
139 indeed comprise only a very small proportion of the total microbial residue (Fig. 3). The ratio of microbial
140 necromass to living biomass is quite stable across biomes in topsoil (Table 1); however, in subsoil this ratio
141 was almost two times higher in boreal forest, montane grassland, and wetland compared to other ecosystems
142 (Extended Data Table 1). In topsoil, microbial necromass, on average, is 23 times greater than living biomass,
143 while in subsoils microbial necromass was more than 70 times greater (Table 1, Extended Data Table 1). This
144 highlights the important role microbes play in SOM formation at depth and suggests subsoils may have higher
145 retention of microbial necromass and/or greater microbial growth efficiencies. In both topsoil or subsoil,
146 microbial necromass to living microbial biomass ratios were greater in soils with high SOM (Extended Data
147 Fig. 8), indicating potentially greater turnover rates of living biomass and/or retention of microbial necromass
148 in OM-rich soils.

149

150 **Limitation and prospects**

151 There are very few studies reporting amino sugars in important SOM storage ecosystems such as tundra,
152 wetlands, permafrost. Our data suggest cold temperatures may limit microbial necromass C accrual in SOM,
153 which may mean that boreal and tundra ecosystems could potentially accrue more microbial necromass C
154 under climate warming, with resulting increases in microbial growth and biomass turnover, and accelerated
155 formation microbial necromass-mineral associations [30] or warming may decrease microbially derived SOM
156 [31]. More research is needed to examine how these vulnerable ecosystems will respond to climate change. Our
157 results show the importance of microbial necromass in subsoil and a general lack of data, highlighting the

need for more studies that include subsoil or are focused on subsoil with regard to microbial necromass and SOM.

With the development of isotopic and spectroscopy techniques, there is a wide recognition that microbial residues are a critical component of stabilized SOM, however, microbial necromass has not been adequately represented in most microbial explicit or general SOM models. Only recently researchers attempted to incorporate microbially derived C into models to show they did indeed perform better than existing models [8]. However, due to limited observation data and no quantitative constraints at global scale, their estimation of microbial necromass C within total SOC were much lower than previous [3] and our current estimates. The data set presented here can serve as a benchmark for biogeochemical and earth systems models to parameterize and more accurately estimate and constrain microbial necromass contributions to SOM, which is a fundamental step for the improvement of nutrient management in agroecosystems and for mitigating soil degradation and climate change.

## References


1. Lehmann, J., Bossio, D. A., Kögel-Knabner, I. & Rillig, M. C. The concept and future prospects of soil health. *Nat. Rev. Earth Environ.* **1**, 544–553 (2020).

2. Paustian, K. *et al.* Climate-smart soils. *Nature* **532**, 49–57 (2016).

3. Liang, C., Amelung, W., Lehmann, J. & Kästner, M. Quantitative assessment of microbial necromass contribution to soil organic matter. *Glob. Chang. Biol.* **25**, 3578–3590 (2019).

4. Lehmann, J. & Kleber, M. The contentious nature of soil organic matter. *Nature* **528**, 60–68 (2015).

5. Miltner, A., Bombach, P., Schmidt-Brücken, B. & Kästner, M. SOM genesis: Microbial biomass as a significant source. *Biogeochemistry* **111**, 41–55 (2012).

6. Schmidt, M. W. I. *et al.* Persistence of soil organic matter as an ecosystem property. *Nature* **478**, 49–56 (2011).

7. Grandy, A. S. & Neff, J. C. Molecular C dynamics downstream: The biochemical decomposition sequence and its impact on soil organic matter structure and function. *Sci. Total Environ.* **404**, 297–307 (2008).

8. Fan, X. Improved model simulation of soil carbon cycling by representing the microbially derived organic carbon pool. *ISME J.* (2021). doi:10.1038/s41396-021-00914-0

9. Angst, G., Mueller, K. E., Nierop, K. G. J. & Simpson, M. J. Plant- or microbial-derived ? A review on the molecular composition of stabilized soil organic matter. *Soil Biol. Biochem.* **156**, 108189 (2021).

10. Joergensen, R. G. Amino sugars as specific indices for fungal and bacterial residues in soil. *Biol. Fertil. Soils* **54**, 559–568 (2018).

11. Chen, G. *et al.* Patterns and determinants of soil microbial residues from tropical to boreal forests. *Soil Biol. Biochem.* **151**, 108059 (2020).

12. Wang, X. *et al.* Elevated temperature increases the accumulation of microbial necromass nitrogen in soil via increasing microbial turnover. *Glob. Chang. Biol.* **26**, 5277–5289 (2020).

13. Hall, S. J., Ye, C., Weintraub, S. R. & Hockaday, W. C. Molecular trade-offs in soil organic carbon composition at continental scale. *Nat. Geosci.* **13**, 687–692 (2020).

14. Sokol, N. W. & Bradford, M. A. Microbial formation of stable soil carbon is more efficient from belowground than aboveground input. *Nat. Geosci.* **12**, 46–53 (2019).

15. Simpson, A., Simpson, M., Smith, E. & Brian, K. Microbially derived inputs to soil organic matter: Are current estimates too low? *Environ. Sci. Technol.* **41**, 8070–8076 (2007).

16. Stevenson, F. J. Organic forms of nitrogen. in *Nitrogen in agricultural soils* 67–122 (1982).

17. Rillig, M. C., Caldwell, B. A., Wösten, H. A. B. & Sollins, P. Role of proteins in soil carbon and nitrogen storage: Controls on persistence. *Biogeochemistry* **85**, 25–44 (2007).

18. Miltner, A., Kindler, R., Knicker, H., Richnow, H. H. & Kästner, M. Fate of microbial biomass-derived amino acids in soil and their contribution to soil organic matter. *Org. Geochem.* **40**, 978–985 (2009).

19. Kallenbach, C. M., Frey, S. D. & Grandy, A. S. Direct evidence for microbial-derived soil organic matter formation and its ecophysiological controls. *Nat. Commun.* **7**, 1-10 (2016).

20. Adamczyk, B., Sietiö, O. M., Biasi, C. & Heinonsalo, J. Interaction between tannins and fungal necromass stabilizes fungal residues in boreal forest soils. *New Phytol.* **223**, 16–21 (2019).

21. Fernandez, C. W., Langley, J. A., Chapman, S., McCormack, M. L. & Koide, R. T. The decomposition of ectomycorrhizal fungal necromass. *Soil Biol. Biochem.* **93**, 38–49 (2016).

22. Bahram, M. *et al.* Structure and function of the global topsoil microbiome. *Nature* **560**, 233–237 (2018).

23. Steidinger, B. S. *et al.* Climatic controls of decomposition drive the global biogeography of forest-tree symbioses. *Nature* **569**, 404–408 (2019).

24. Pietikäinen, J., Pettersson, M. & Bååth, E. Comparison of temperature effects on soil respiration and bacterial and fungal growth rates. *FEMS Microbiol. Ecol.* **52**, 49–58 (2005).

25. Cotrufo, M. F., Wallenstein, M. D., Boot, C. M., Denef, K. & Paul, E. The Microbial Efficiency-Matrix Stabilization (MEMS) framework integrates plant litter decomposition with soil organic matter

stabilization: Do labile plant inputs form stable soil organic matter? *Glob. Chang. Biol.* **19**, 988–995 (2013).

26. Jones, D. L., Cooledge, E. C., Hoyle, F. C., Griffiths, R. I. & Murphy, D. V. pH and exchangeable aluminum are major regulators of microbial energy flow and carbon use efficiency in soil microbial communities. *Soil Biol. Biochem.* **138**, 107584 (2019).

27. Rousk, J., Brookes, P. C. & Bååth, E. Contrasting soil pH effects on fungal and bacterial growth suggest functional redundancy in carbon mineralization. *Appl. Environ. Microbiol.* **75**, 1589–1596 (2009).

28. Soares, M. & Rousk, J. Microbial growth and carbon use efficiency in soil: Links to fungal-bacterial dominance, SOC-quality and stoichiometry. *Soil Biol. Biochem.* **131**, 195–205 (2019).

29. Xu, X., Thornton, P. E. & Post, W. M. A global analysis of soil microbial biomass carbon, nitrogen and phosphorus in terrestrial ecosystems. *Glob. Ecol. Biogeogr.* **22**, 737–749 (2013).

30. Tian, J. *et al.* Microbial metabolic response to winter warming stabilizes soil carbon. *Glob. Chang. Biol.* **27**, 2011-2028 (2021).

31. Liang, C. & Balser, T. C. Warming and nitrogen deposition lessen microbial residue contribution to soil carbon pool. *Nat. Commun.* **3**, 23–26 (2012).

**Table 1. Microbial necromass stocks and contributions to soil organic matter in topsoil (0-30 cm) across different biomes**.

| Biomes | Area (million $km^{-2}$) | Necromass-C (Gt) | Necromass-N (Gt) | Necromass-C/SOC (%) | Necromass-N/TN (%) | FC/BC | FN/BN | Necromass C/MBC | Necromass N/MBN |
|---|---|---|---|---|---|---|---|---|---|
| Tropical & subtropical forests | 18.0 | 41.0 | 6.3 | 38.9 | 74.0 | 1.8 | 1.9 | 22.2 | 19.8 |
| Temperate forests | 10.6 | 32.0 | 4.9 | 44.9 | 90.6 | 4.7 | 4.9 | 29.9 | 27.3 |
| Boreal forests/Taiga | 14.8 | 73.7 | 11.3 | 38.2 | 87.6 | 3.9 | 4.1 | 28.7 | 32.9 |
| Tropical & subtropical grasslands, savannas & shrublands | 17.2 | 27.9 | 4.3 | 52.8 | 84.6 | 2.9 | 3.1 | 21.4 | 19.7 |
| Temperate grasslands, savannas & shrublands | 5.1 | 12.2 | 1.9 | 59.8 | 91.5 | 2.5 | 2.6 | 24.5 | 28.4 |
| Montane grasslands & shrublands | 4.5 | 8.3 | 1.3 | 53.3 | 75.5 | 3.9 | 4.1 | 21.2 | 26.2 |
| Mediterranean forests, woodlands & scrub | 1.9 | 2.8 | 0.4 | 51.1 | 83.4 | 3.1 | 3.3 | 18.4 | 17.2 |
| Deserts & xeric shrublands | 25.8 | 26.3 | 4.0 | 56.6 | 76.4 | 2.9 | 3.0 | 17.5 | 17.2 |
| Tundra | 8.1 | 11.9 | 1.8 | 19.1 | 41.1 | 2.9 | 3.0 | 9.6 | 10.3 |
| Wetlands | 1.1 | 3.9 | 0.6 | 49.8 | 83.4 | 3.1 | 3.3 | 34.9 | 27.1 |
| Croplands | 24.0 | 58.6 | 9.0 | 49.3 | 80.7 | 2.1 | 2.2 | 25.8 | 26.3 |
| Global | 131.1 | 320.6 | 49.3 | 44.4 | 77.2 | 3.0 | 3.1 | 22.6 | 23.0 |

FC/BC, the ratio of fungal necromass C to bacterial necromass C. FN/BN, the ratio of fungal necromass N to bacterial necromass N. NecromassC/MBC, the ratio of microbial necromass C to living microbial biomass C. NecromassN/MBN, the ratio of microbial necromass N to living microbial biomass N.

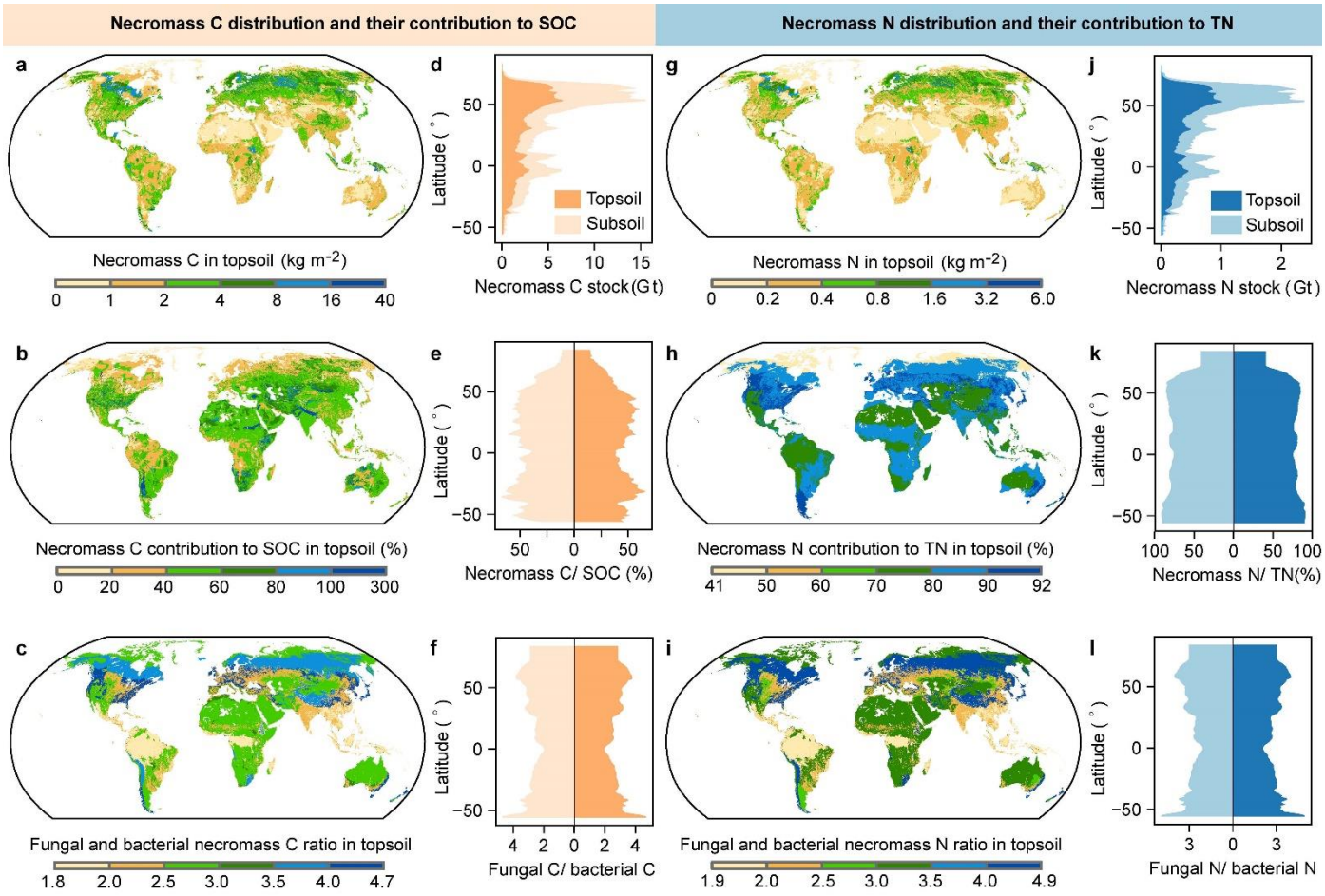


**Fig. 1 Global distributions of microbial necromass, percent necromass contributions to soil organic matter and ratio of fungal to bacterial necromass**. **a-c,** Microbial necromass C distribution (**a**), percent contributions to soil organic carbon (SOC; **b**), and the relative contributions of fungal and bacterial necromass C in topsoil (**c**) and **d-f,** corresponding latitudinal patterns in both topsoil and subsoil. **g-i,** Microbial necromass N distribution (**g**), percent contribution to soil total nitrogen (TN) (**h**), the relative contributions of fungal and bacterial necromass N (**i**) in topsoil, with corresponding latitudinal patterns in topsoil and subsoil (**j-l**). All global maps are 0.083° (~10 km) resolution.

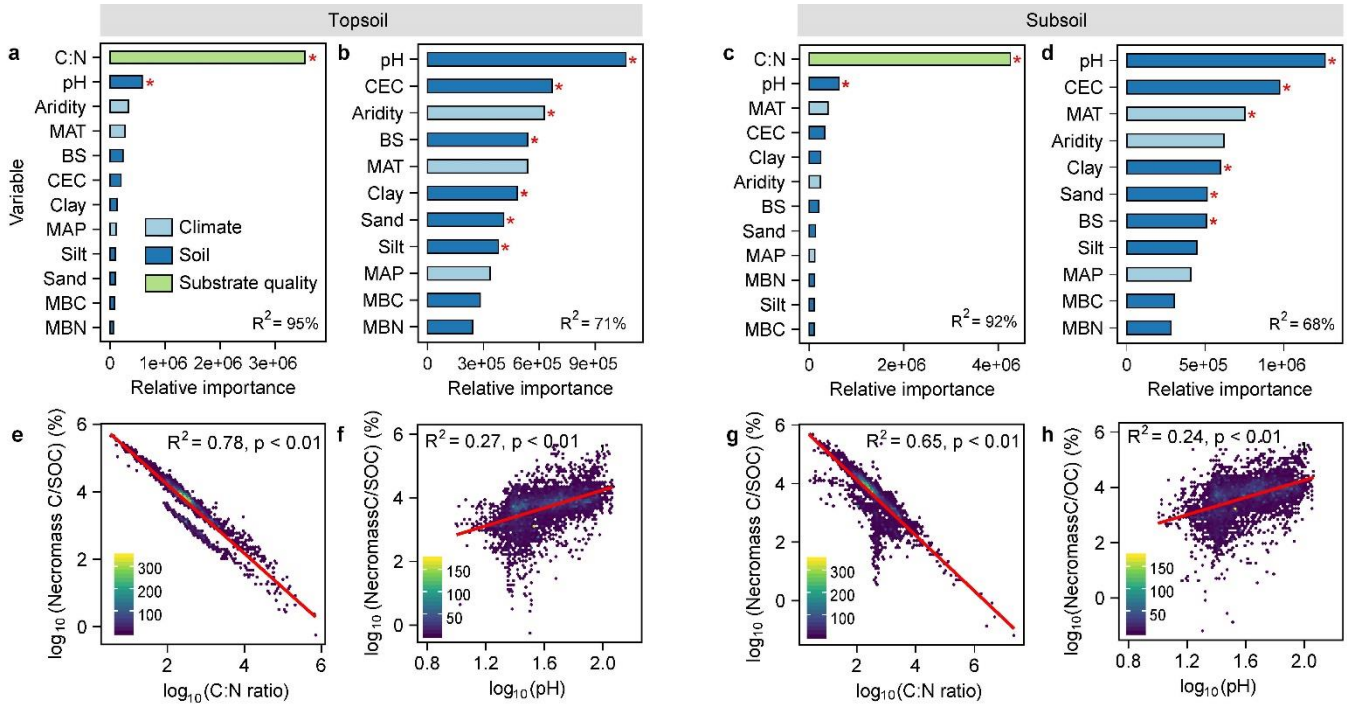


**Fig. 2 Climate factors and soil characteristics that control microbial necromass contributions to SOC in topsoil and subsoil at a global scale. a-d,** Random forest analyses of the relative importance (IncNodePurity) of different variables in relation to microbial necromass C contributions to SOC with and without inclusion of soil C:N ratios in topsoil (**a-b**) and subsoil (**c-d**), respectively. Red asterisks indicate significant influence at $P < 0.05$. **e-h,** Relationships between soil C:N ratios or soil pH and microbial necromass C contributions to SOC in topsoil (**e-f**) and subsoil (**g-h**). Relationships are based on data from 10,000 randomly sampled pixels across the globe and all data were log-transformed. MAT: mean annual temperature, MAP: mean annual precipitation, pH: soil pH measured by potassium chloride, BS: base saturation, CEC: cation exchange capacity, MBC: microbial biomass carbon, MBN: microbial biomass nitrogen.

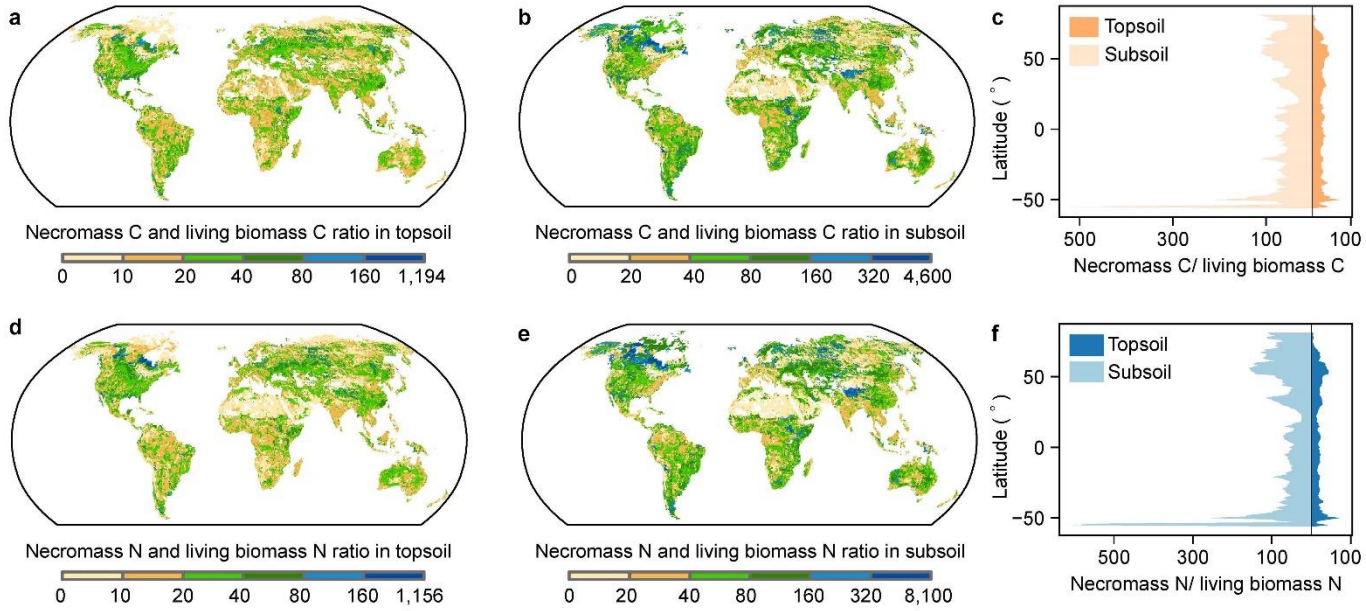


259

260 **Fig. 3 Spatial patterns of the ratio of microbial necromass to living microbial biomass**. **a-c,** Distribution of the
261 ratio of microbial necromass C to living microbial biomass C in topsoil (**a**), subsoil (**b**), and the corresponding
262 latitudinal patterns (**c**). **d-f**, Distribution of the ratio of microbial necromass N to living microbial biomass N in topsoil
263 (**d**), subsoil (**e**), and their corresponding latitudinal patterns (**f**). All global maps are 0.083° (~10 km) resolution.

264

## Methods

### Data collection

We first compiled literature that reported the concentration of amino sugars from Web of Science (http://apps.webofknowledge.com) and China National Knowledge Infrastructure (http://www.cnki.net) before 2021 January, with the key words of 'amino sugar' and 'microbial necromass'. Data were compiled following the below criteria:

1) Total amino sugar was clearly reported even if glucosamine or muramic acid were not available.
2) Corresponding soil organic C concentrations must be reported to calculate microbial necromass contribution to SOC.
3) Laboratory incubation studies were not included unless the data from time zero at control condition without any treatment were included.
4) Pot experiments were not included unless a time zero control could be used.
5) Experiments with artificial soils were not included.
6) Only data from mineral soils were included, data from organic or litter layers were not included.
7) Only data from bulk soil were included, data in different aggregate fractions were not included.
8) The same results presented in different publications by the same research group were included only once in our dataset.
9) Only data from control plots or undisturbed soils were used in natural ecosystem studies (such as forest, grassland, wetland).

Data presented in the figures were extracted by the free software of GETDATA GRAPH DIGITIZER (http://getdata-graph-digitizer.com). In addition, site vegetation type, basic information (latitude, longitude, elevation), mean annual temperature (MAT), mean annual precipitation (MAP), soil basic properties [soil organic carbon (SOC), total nitrogen (TN), C: N ratio, pH, texture (sand, silt, clay), microbial biomass carbon (MBC) and microbial biomass nitrogen (MBN)] were also collected if they were reported. Finally, we compiled 902 observations from 119 peer-reviewed papers and our own data, which come from forest (212), grassland (248), and cropland (407) ecosystems across different climate regions, while other ecosystems (xeric desert, wetland, tundra, etc.) all together have only 35 total observations. Overall, these observations from

28 °S to 70 °N latitude, range in annual mean precipitation from 19 to 2942 mm, and in annual mean temperature from -11 to 32°C (Extended Data Fig. 1).

**Missing amino sugar data filling**

There were around 120 measurements reporting total amino sugar while not reporting glucosamine or muramic acid (Supplement Data1). We found a strong relationship between different amino sugar compounds (glucosamines, galactosamine, muramic acid, mannosamine) and total amino sugar (with $R^2$ range from 0.83 to 0.98, Extended Data Fig. 2a-d). In addition, our results showed that glucosamine (GluN) and galactosamine (GlaN) are the major components of total amino sugars, while muramic acid (MurA) and mannosamine (ManN) only comprise a small proportion of the total amino sugar (Extended Data Fig. 2e), consistent with previous work [10]. In order increase the available data, we first filled in the data sets missing glucosamines and muramic acid cases based on the strong relationships with total amino sugars (Extended Data Fig. 2).

**Amino sugar prediction based on machine learning methods**

Based on the complied dataset, we first conducted a correlation analysis between amino sugar with climate (MAT and MAP), and edaphic properties (SOC, TN, C:N ratio, pH, sand, silt, clay, MBC, and MBN) using *corrplot* package in R (http://cran.r-project.org/). Then we conducted a random forest analysis to identify the main predictors for the amino sugar. The importance of each predictor variable is determined by evaluating the decrease in prediction accuracy (that is, increase in the mean square error between observations and predictions) when the data for that predictor is randomly permuted [32]. This accuracy importance measure was computed for each tree and averaged over the forest (5,000 trees). Random forest analyses were conducted using the *randomForest* package in R. In addition, the significance of the importance of each predictor on amino sugar was assessed by using the *rfPermute* package in R. Random forest analysis results explained 74.3% to 87.6% of the variance for different amino sugars. Besides, random forest analysis suggested that TN and SOC were the two most significant predictors for different amino sugars (Extended Data Fig. 3b). Then we built a linear mixing model using *nlme* package in R to compare different model performance that include TN,

SOC, as well as MAT and MAP. Linear mixing model results showed that models contain TN only is enough to predict the variation of amino sugar, models that adding more variables did not significantly improve prediction of the amino sugar variation (Extended Data Fig. 3c). Therefore, in the following analysis, we only used TN as the predictor for amino sugar to simplify the prediction model. $R^2$ of the prediction model with TN in different ecosystems varied from 0.74 to 0.94 for total amino sugar (TAS), 0.74 to 0.94 for GluN, and 0.74 to 0.95 for MurN, respectively (Extended Data Fig. 3d). Overall, TN explained 91% of the variation for TAS, 90% variation for GluN, and 79% variation for MurA, respectively (Extended Data Fig. 3e).

**Climate, soil edaphic properties, microbial biomass data**

SOC, TN, bulk density, gravel content, pH (extracted by KCl), soil texture (sand, silt, clay), cation exchange capacity (CEC), and base saturation (BS) were obtained from gridded Global Soil Dataset (GSDE) to the depth of 1.0 m at a 0.083° spatial resolution (http://globalchange.bnu.edu.cn/research/soilw) [33]. Average MAT and MAP for 1970-2000 years were obtained from the WorldClim database version 2 at the spatial resolution of 30 arc-seconds (https://www.worldclim.org/data/worldclim21.html). Aridity index were obtained from the Global Aridity and PET Database (https://cgiarcsi.community/data/global-aridity-and-pet-database). Global microbial biomass C and N from topsoil (0-30 cm) and subsoil (30-100 cm) at a 0.05° spatial resolution were obtained from a global microbial biomass dataset (https://daac.ornl.gov/SOILS/guides/Global_Microbial_Biomass_C_N_P) [29].

**Global vegetation cover (biome) data**

The global map of biome types were generated by merging two land cover maps: the MODIS land cover map (https://globalmaps.github.io/glcnmo.html#summary) and the WWF (World Wildlife Fund) map of the Terrestrial Ecoregions of the World49 (https://www.worldwildlife.org/publications/terrestrial-ecoregions-of-the-world).The two maps are aggregated to generate a biome map having the same resolution (0.083°) of soil edaphic properties and were reclassified into 11 biomes (Extended Data Fig. 1a): tropical/subtropical forests (01), temperate forests (02), boreal forests/Taiga (03), tropical/subtropical grasslands/savannas & shrublands

(04), temperate grasslands, savannas & shrublands (05), montane grasslands & shrublands (06), Mediterranean forest woodland & scrub (07), desert & xeric shrublands (07), tundra (09), wetlands (10), and croplands (11).

**Conversion of amino sugar into microbial necromass**

Amino sugar biomarkers have been widely applied to trace the microbial origin of SOC [10]. Muramic acid (MurN) occurs exclusively in the murein layers of bacterial cell walls, while fungal cell walls are the major source of glucosamine (GluN) in soil [34]. Based on assumption that MurN and GluN occur at a molar of 1 to 2 ratio in bacteria, fungal GluN can be calculated [10]. Bacteria necromass C can be converted by a factor of 45 from MurN and fungal necromass C can be converted by a factor of 9 by fungal GluN [34]. Therefore, bacterial necromass C and fungal necromass C were calculated by the following formula:

$$\text{Bacterial necromass C} = \text{MurA} \cdot 45 \quad (1)$$

$$\text{Fungal necromass C} = (\text{GluN}/179.17 - 2 \cdot \text{MurA}/251.23) \cdot 179.17 \cdot 9 \quad (2)$$

Based on elemental carbon–nitrogen stoichiometry, GluN and MurN can be further converted to bacterial-derived N and fungal-derived N, with average conversion factor of 6.67 and 1.4, respectively [3]. Therefore, bacterial necromass N and fungal necromass N were calculated by the following formula:

$$\text{Bacterial necromass N} = \text{MurA} \cdot 6.67 \quad (3)$$

$$\text{Fungal necromass N} = (\text{GluN}/179.17 - 2 \cdot \text{MurA}/251.23) \cdot 179.17 \cdot 1.4 \quad (4)$$

Microbial necromass C and N was calculated as the sum of fungal and bacterial necromass C and N.

**Calculation of amino sugar and microbial necromass stock**

In this study, at each pixel, we estimated the amino sugar stocks (ASs, kg $m^{-2}$) as well as microbial necromass C and N (MNs, kg $m^{-2}$) for topsoil (0-30 cm) and subsoil (30-100 cm) with the following equation:

$$AS_S = \sum_{1}^{n} AS_n \cdot BD_n \cdot D_n \cdot \left(1 - \frac{G_n}{100}\right) \cdot 10 \quad (5)$$

$$MN_S = \sum_{1}^{n} MN_n \cdot BD_n \cdot D_n \cdot \left(1 - \frac{G_n}{100}\right) \cdot 10 \quad (6)$$

where $AS_n$ and $MN_n$ are the amino sugar and microbial (both fungal and bacterial) necromass concentration (mg $kg^{-1}$), respectively, in each layer, $BD_n$ is the soil bulk density (g $cm^{-3}$) in each layer, $D_n$ is the soil thickness (cm) in each layer, and $G_n$ is the gravel content reported as the percentage of soil volume in each layer, 10 is the conversion factor.

Finally, microbial necromass C to SOC or microbial necromass N contribution to TN were calculated by dividing the SOC or TN by microbial necromass C or N, respectively. Furthermore, we used a range of different global climate and soil properties datasets to identify the driving factors for the microbial necromass contribution to SOM. Since microbial necromass N were estimated by TN, therefore, we only provide a rough estimation of the microbial necromass N contribution to TN in different biomes and only analyzed the factors that affect the microbial neromass C contribution to SOC. In addition, we also estimated the ratio of microbial biomass C and N with living microbial biomass C and N data obtained from [29] for both topsoil and subsoil, which can be used as an indicator of microbial retention efficiency from microbial biomass into stabilized microbial necromass.

**Drivers of microbial necromass contribution to SOM at global scale**

We conducted a random forest analysis to identify the relative importance of climate (MAT, MAP, Aridity), and soil edaphic properties (C:N ratio, pH, MBC, MBN, CEC, BS) in controlling the microbial necromass contribution to SOC in topsoil and subsoil, respectively. First, we randomly selecting 10,000 pixels of each variables across the globe to reduce the computing time [35]. The importance of each predictor variable is determined by evaluating the decrease in prediction accuracy (that is, the mean node impurity between observations and predictions) when the data for that predictor is randomly permuted for 500 times. Random forest analyses were conducted using the *randomForest* package in R, and the significance of the importance

of each predictor on amino sugar was assessed by using the *rfPermute* package in R.

## Data availability

All data supporting the findings of this study are in Supplementary Information. We will deposit these data in DRYAD after this manuscript have been accepted.

## Code availability

The R code used to generate the results are available from the corresponding authors upon reasonable request (liuyua14@msu.edu).

## Methods references


32. Delgado-Baquerizo, M. *et al.* Microbial diversity drives multifunctionality in terrestrial ecosystems. *Nat. Commun.* **7**, 1–8 (2016).

33. Shangguan, W., Dai, Y., Duan, Q., Liu, B. & Yuan, H. A global soil data set for earth system modeling. *J. Adv. Model. Earth Syst.* **6**, 513–526 (2014).

34. Appuhn, A. & Joergensen, R. G. Microbial colonisation of roots as a function of plant species. *Soil Biol. Biochem.* **38**, 1040–1051 (2006).

35. Luo, Z., Wang, G. & Wang, E. Global subsoil organic carbon turnover times dominantly controlled by soil properties rather than climate. *Nat. Commun.* 1–10 (2019).


## Acknowledgements


We thank H. Yu, University of Twente, for help with spatial analyses, and G.P. Robertson and members of the Soil Biology Lab at Michigan State University for comments on previous versions of the manuscript. This work was supported by awards from the U.S. Department of Energy, Office of Science, Office of Biological

and Environmental Research award DE-SC0014108 to L.K.T.; the National Science and Technology Basic Resources Survey Program of China (2019FY101300) to N.H. and the National Natural Science Foundation of China (32071629) and National Key R&D Program of China (2017YFA0604803) to J.T.

## Author contributions

Y.L., L.K.T., J.T. and N.H. conceived the study. Y.L. extracted data from the literature, compiled the database and performed data analyses. J.T. provided 52 non-published amino sugar datasets from Chinese grasslands and forests and N.H. provided the other corresponding soil properties. Y.L. and L.K.T. wrote the manuscript with contributions from all authors.

## Competing interests

The authors declare no competing interests.

## Additional information

**Supplementary information** is available for this paper.

**Correspondence and requests for materials** should be addressed to Y.L. (liuyua14@msu.edu) or L.K.T. (ltiemann@msu.edu).

# Extended figures and tables

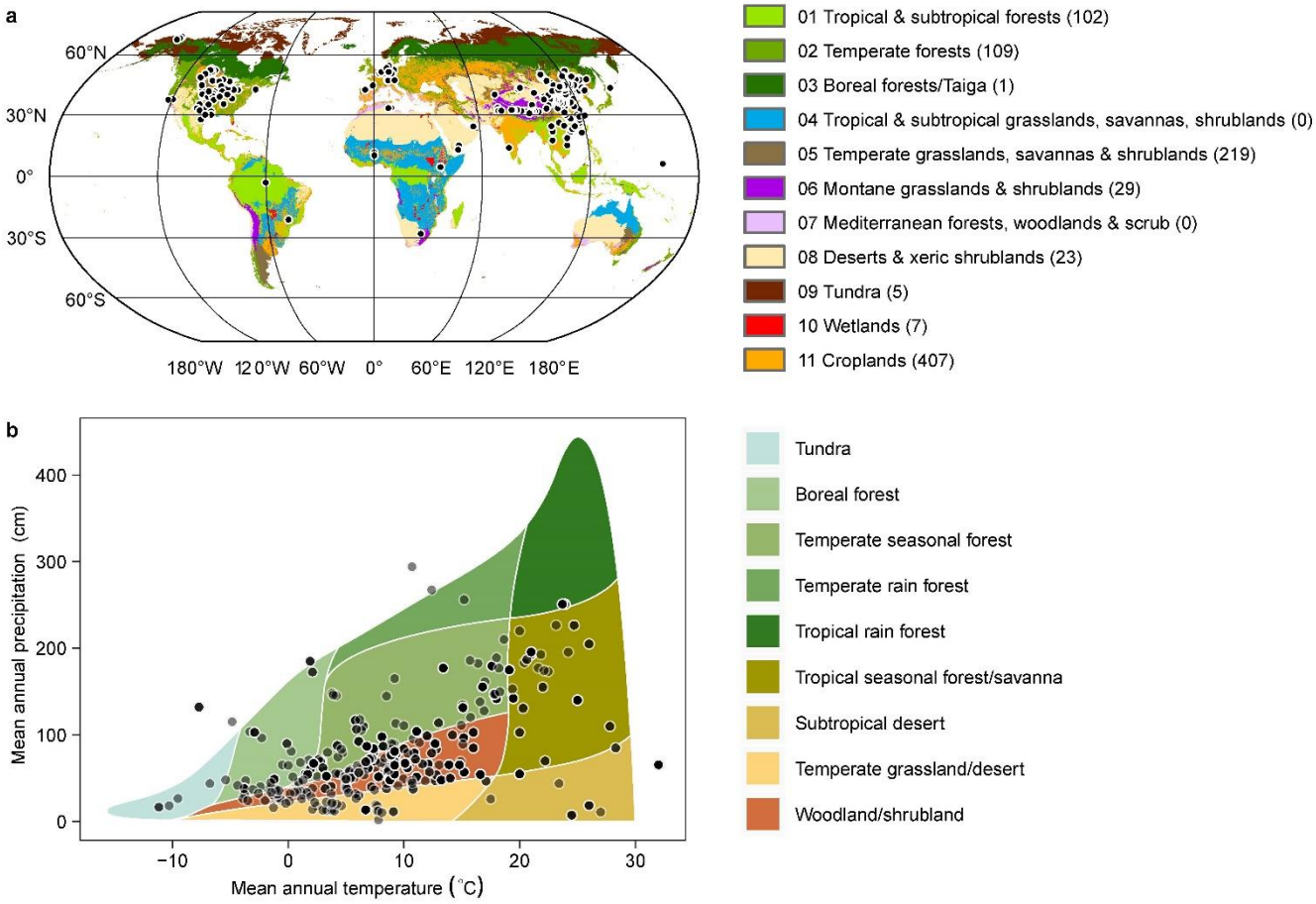


**Extended Data Fig. 1 Soil amino sugar data distribution across biomes and climates**. We collected a total of 902 soil amino sugar measurements made in either topsoil (0-30 cm) or subsoil (30-100 cm) spanning all major land cover types (**a**) and climate zones (**b**). These data were used to build the relationship(s) with soil TN, that could then be used to extrapolate global amino sugar stocks.

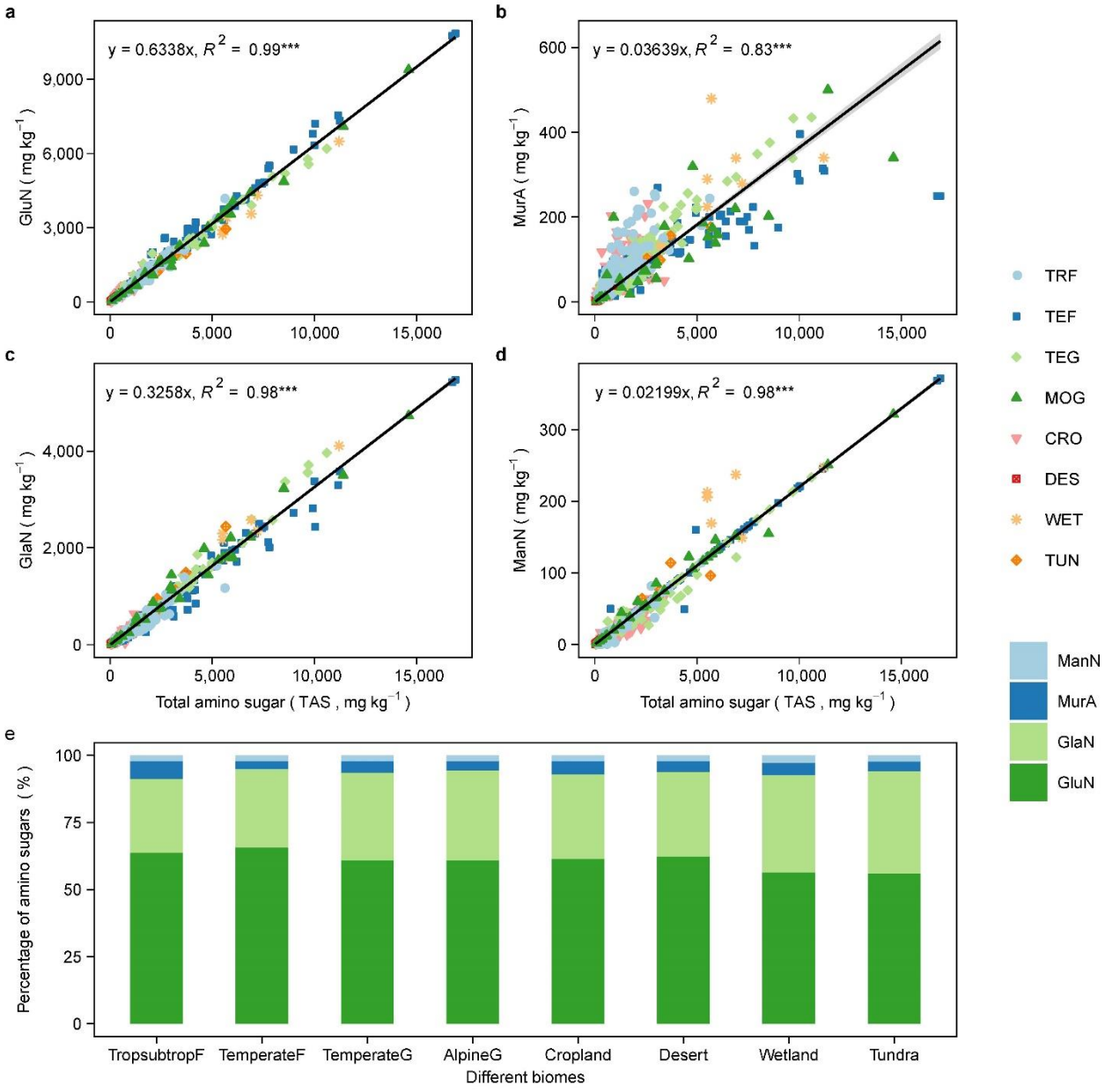


**Extended Data Fig. 2 Relationship between different amino sugar components and total amino sugar**. **a-d,** Strong relationships between total amino sugar (TAS) and different amino sugar components, glucosamine (GluN, **a**), muramic acid (MurA, **b**), galactosamine (GlaN, **c**) and mannosamine (ManN, **d**) were used to fill missing amino sugar data where only total amino sugar data were reported (n = 782). The reported fractions of different amino sugar components relative to total amino sugars indicate that GluN and GlaN are the major component of amino sugars, while MurA and ManN only comprise a small proportion of total amino sugars. Grey shading around regression lines represents 95% confidence intervals, with asterisks after $R^2$ values indicating significant effects ($P < 0.001$). TRF: Tropical & subtropical forests, TEF: Temperate forests, TEG: Temperate grasslands, savannas & shrublands, MOG: Montane grasslands & shrublands, DES: Deserts & xeric shrublands, TUN: Tundra, WET: Wetlands, CRO: Croplands.

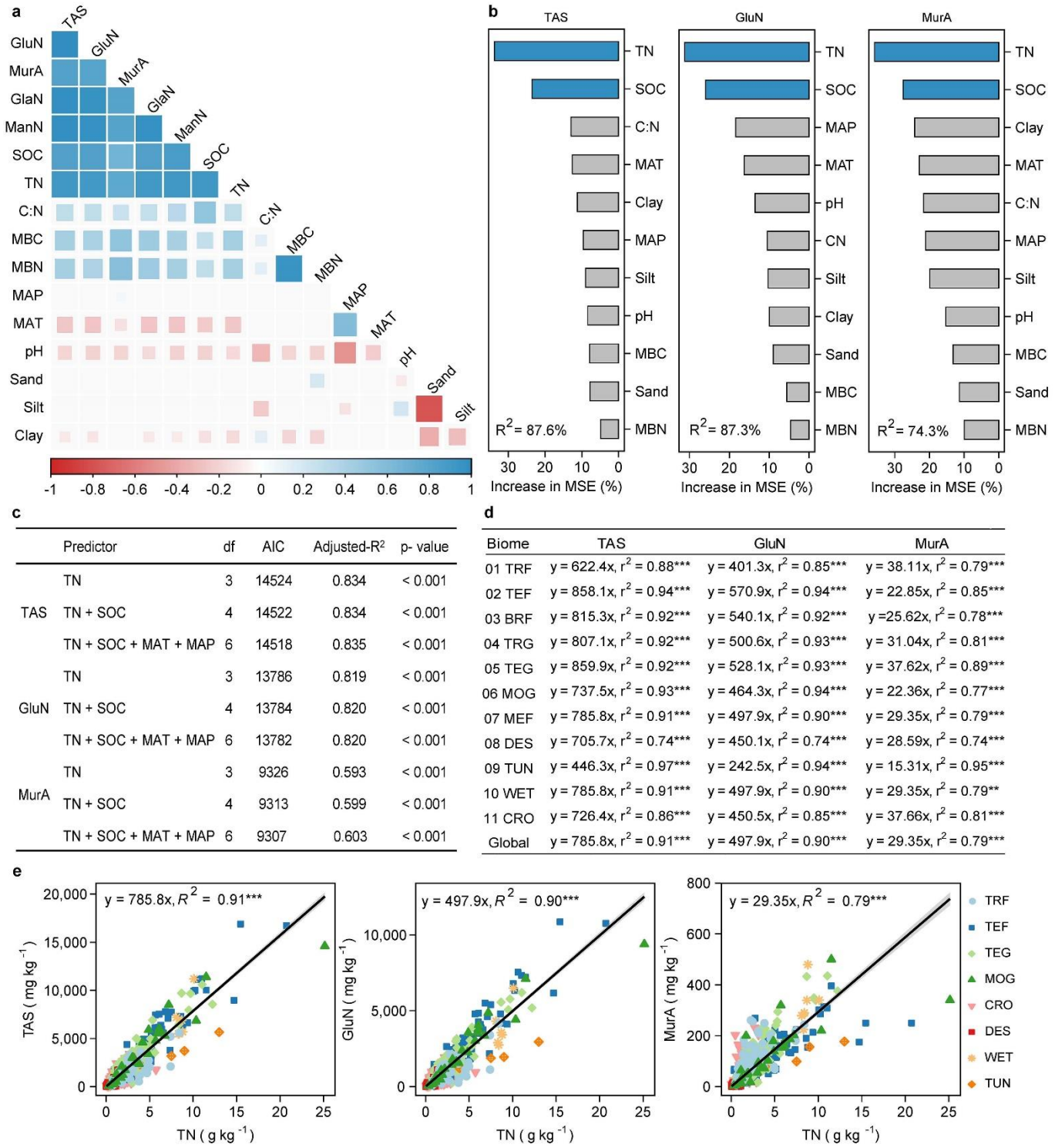


**Extended Data Fig. 3 Relationships between amino sugars and different climate factors and soil characteristics.** **a**, Pearson correlation matrix between amino sugars and different predictor variables (n = 902). **b**, Relative importance of different variables for predicting the amino sugars from random forest analysis, with significant variables in blue bar at $P < 0.05$. **c**, Linear mixing model analyses used to predict different amino sugars with different variables (n = 902). **d**, Prediction model of total amino sugars (TAS), glucosamine (GluN), and muramic acid (MurA) based on soil total nitrogen (TN) in each biome, with **, *** indicating significant effects at $P < 0.01$ and $P < 0.001$, respectively. **e**, Correlations between different amnio sugars with predicting variable (TN) selected from random forest and linear mixing model analysis (n = 902). Grey shading around regression lines represents 95% confidence intervals, with asterisks indicating significant effects ($P < 0.001$). SOC: soil organic carbon, MBC: microbial biomass carbon, MBN: microbial biomass nitrogen, MAT: mean annual temperature, MAP: mean annual precipitation, pH: soil pH. TRF: Tropical & subtropical forests, TEF: Temperate forests, BRF, Boreal forest/Taiga, TRG: Tropical & subtropical grasslands, savannas & shrublands, TEG: Temperate grasslands, savannas & shrublands, MOG: Montane grasslands & shrublands, MEF: Mediterranean forests, woodlands & scrub, DES: Deserts & xeric shrublands, TUN: Tundra, WET: Wetlands, CRO: Croplands.

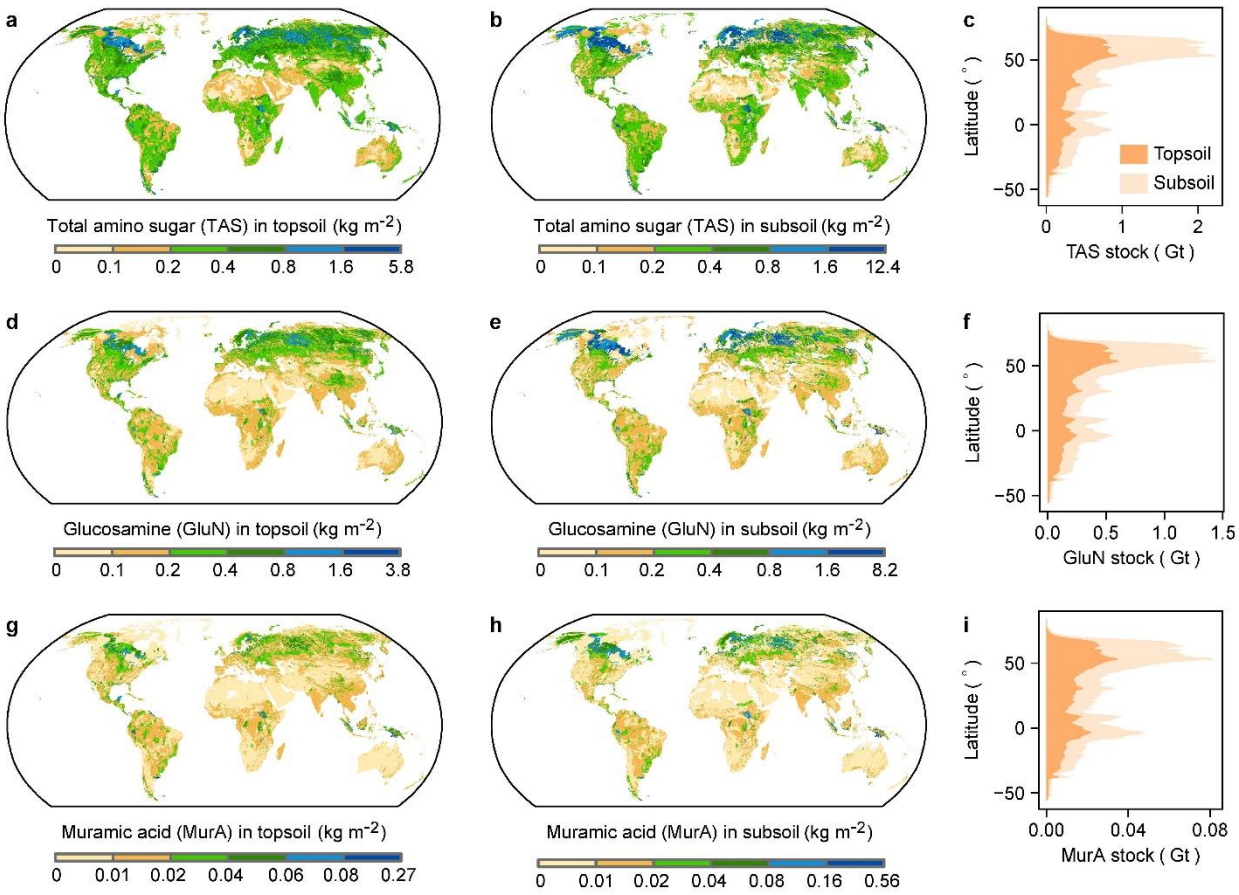


**Extended Data Fig. 4 Global distribution of soil amino sugar. a**, Global distribution of total amino sugar (TAS) in topsoil (0-30 cm). **b**, Global distribution of TAS in subsoil (30-100 cm). **c**, TAS latitudinal patterns in topsoil and subsoil. **d**, Global distribution of glucosamine (GluN) in topsoil (0-30 cm). **e**, Global distribution of GluN in subsoil (30-100 cm). **f**, GluN latitudinal patterns in topsoil and subsoil. **g**, Global distribution of glucosamine (MurA) in topsoil (0-30 cm). h, Global distribution of MurA in subsoil (30-100 cm). **i**, MurA latitudinal patterns in topsoil and subsoil. All global maps are 0.083° (~10 km) resolution.

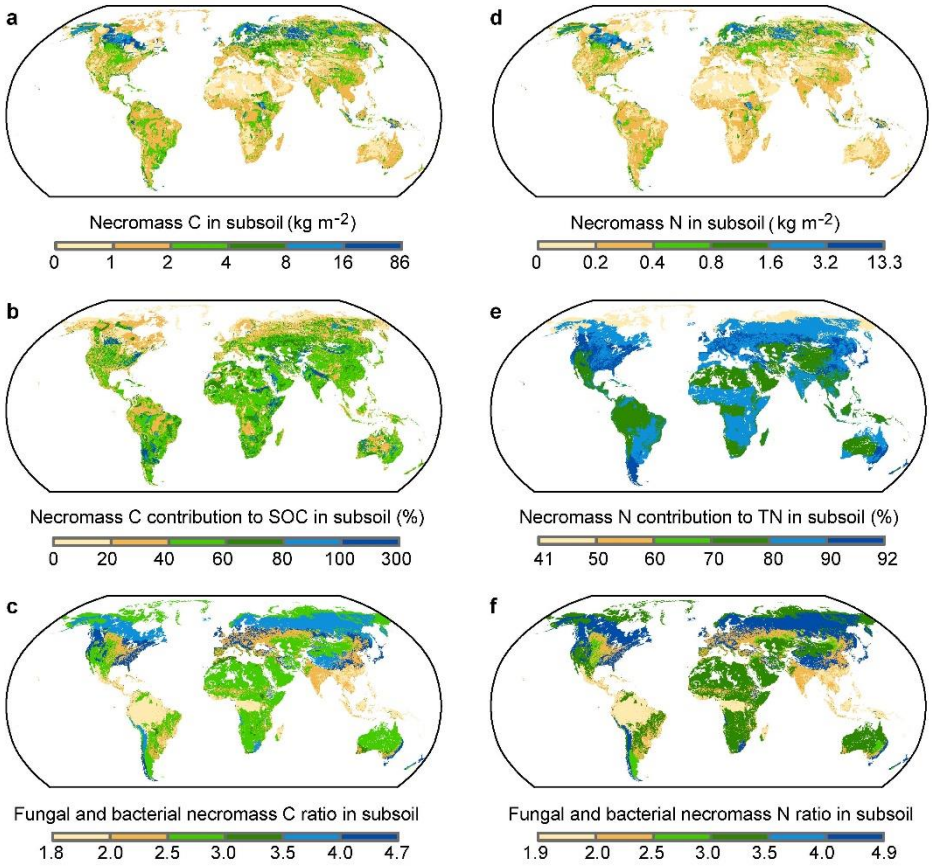


**Extended Data Fig. 5 Global distribution of subsoil microbial necromass and contributions to soil organic matter**. **a-c,** Microbial necromass C distribution (**a**), its contribution to soil organic carbon (SOC) (**b**), and the relative contribution of fungal and bacterial necromass C (**c**) in subsoil (30-100 cm). **d-f,** Microbial necromass N distribution (**d**), its contribution to TN (**e**), and the relative contribution of fungal and bacterial necromass N (**f**) to subsoil (30-100 cm). All global maps are 0.083° (~10 km) resolution.

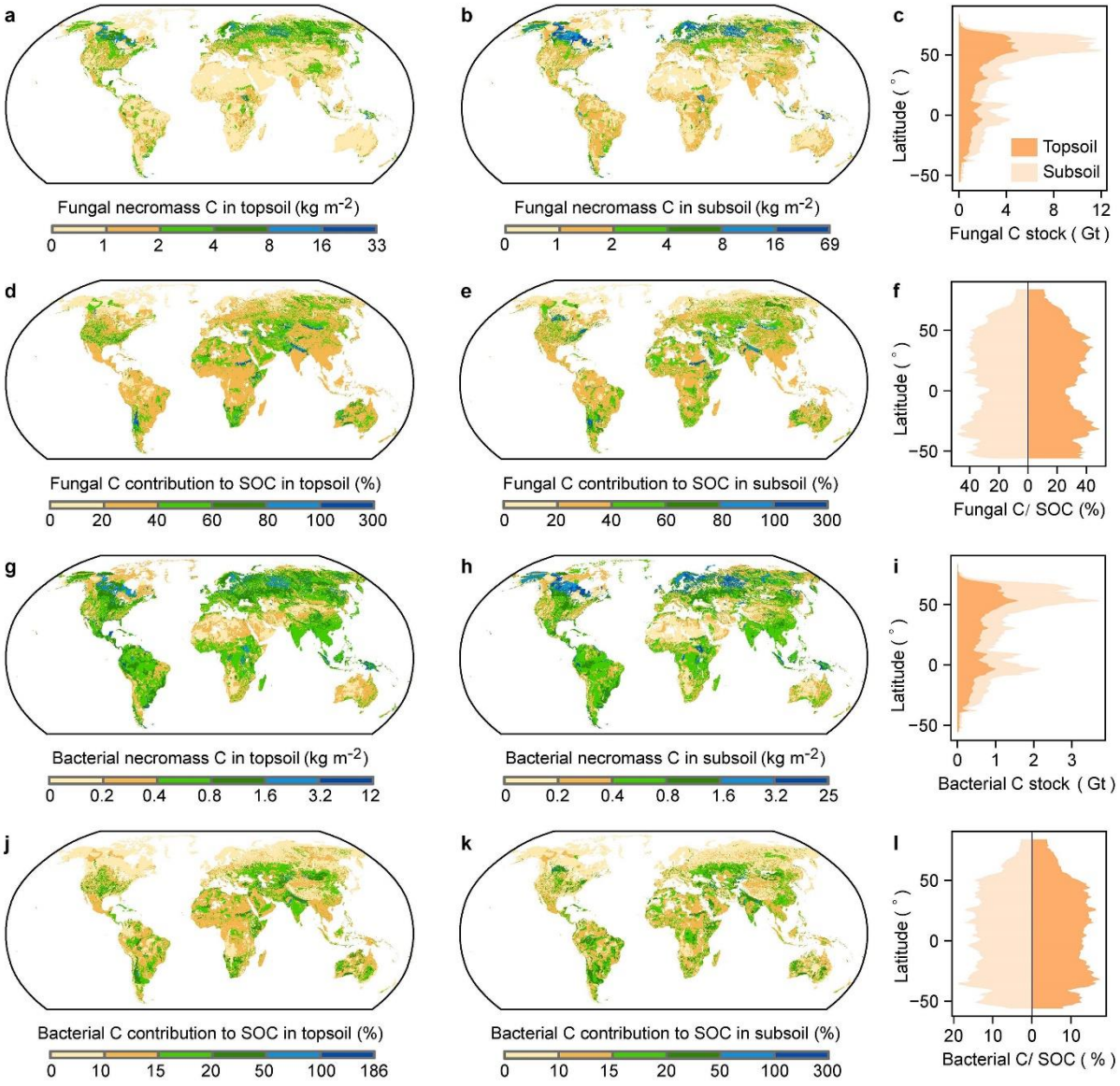


**Extended Data Fig. 6 Global distribution of fungal and bacterial necromass C and their contribution to soil organic carbon (SOC). a-c,** Global distribution of fungal necromass C in topsoil (**a**), subsoil **(b),** and corresponding latitudinal patterns in topsoil and subsoil (**c**). **d-f,** Global distribution of fungal necromass C contributions to SOC (%) in topsoil (**d**), subsoil **(e),** and corresponding latitudinal patterns in topsoil and subsoil (**f**). **g-i,** Global distribution of bacterial necromass C contribution to SOC in topsoil (**g**), subsoil **(h),** and corresponding latitudinal patterns in topsoil and subsoil (**i**). **j-l,** Global distribution of bacterial necromass C contribution to SOC in topsoil (**j**), subsoil **(k),** and corresponding latitudinal patterns in topsoil and subsoil (**l**). All global maps are 0.083° (~10 km) resolution.

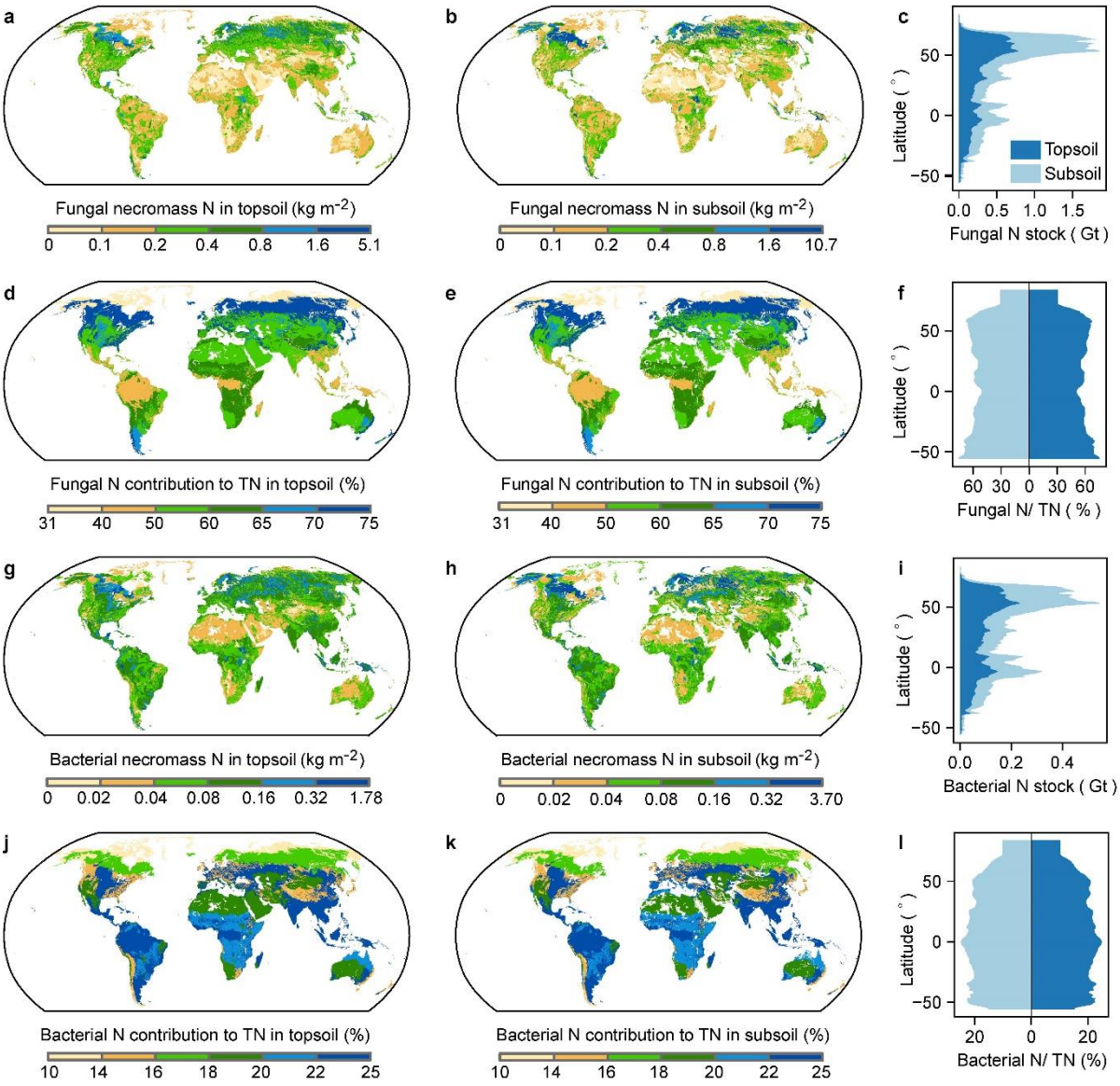


**Extended Data Fig. 7 Global distribution of fungal and bacterial necromass N and their contribution to soil total nitrogen (TN). a-c,** Global distribution of fungal necromass N in topsoil (**a**), subsoil **(b),** and corresponding latitudinal patterns in topsoil and subsoil (**c**). **d-f,** Global distribution of fungal necromass N contribution to TN in topsoil (**d**), subsoil **(e),** and corresponding latitudinal patterns in topsoil and subsoil (**f**). **g-i,** Global distribution of bacterial necromass N contribution to TN in topsoil (**g**), subsoil **(h),** and corresponding latitudinal patterns in topsoil and subsoil (**i**). **j-l,** Global distribution of bacterial necromass N contribution to TN in topsoil (j), subsoil **(k),** and corresponding latitudinal patterns in topsoil and subsoil (**l**). All global maps are 0.083° (~10 km) resolution.

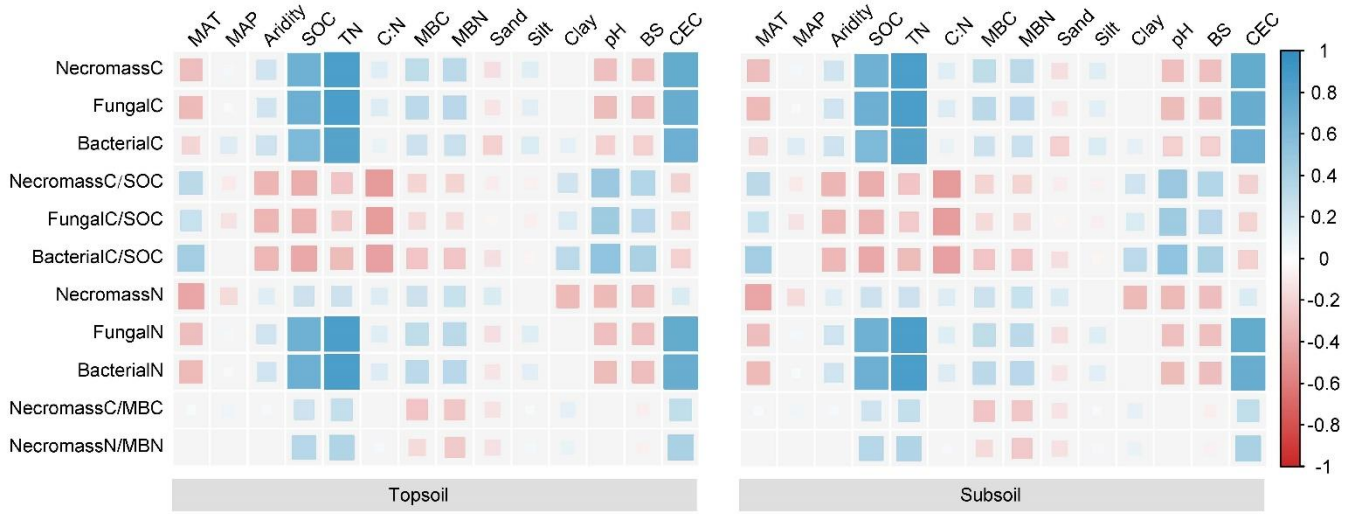


503

504 **Extended Data Fig. 8 Pearson correlation matrix between microbial necromass and necromass contributions to**
505 **soil organic matter with different variables in topsoil (0-30 cm) and subsoil (30-100 cm).** SOC: soil organic
506 carbon, TN, soil total nitrogen, MAT: mean annual temperature, MAP: mean annual precipitation, pH: soil pH
507 measured by potassium chloride, BS: base saturation, CEC: cation exchange capacity, MBC: microbial biomass
508 carbon, MBN: microbial biomass nitrogen.

509

**Extend Data Table 1 Microbial necromass C and N stock, their contribution to soil organic matter in subsoil (30-100 cm) in different biomes**.

| Biomes | Area (million $km^{-2}$) | Necromass C (Gt) | Necromass N (Gt) | NecromassC/s SOC (%) | NecromassN/ TN (%) | FC/ BC | FN/ BN | Necromass C/MBC | Necromass N/MBN |
|---|---|---|---|---|---|---|---|---|---|
| Tropical & subtropical forests | 18.0 | 41.7 | 6.4 | 42.7 | 74.0 | 1.8 | 1.9 | 52.2 | 45.7 |
| Temperate forests | 10.6 | 34.5 | 5.3 | 45.6 | 90.6 | 4.7 | 4.9 | 65.9 | 66.9 |
| Boreal forests/Taiga | 14.8 | 114.3 | 17.6 | 37.7 | 87.6 | 3.9 | 4.1 | 108.9 | 147.9 |
| Tropical & subtropical grasslands, savannas & shrublands | 17.2 | 30.4 | 4.7 | 54.8 | 84.6 | 2.9 | 3.1 | 68.6 | 61.8 |
| Temperate grasslands, savannas & shrublands | 5.1 | 13.4 | 2.1 | 61.0 | 91.5 | 2.5 | 2.6 | 80.6 | 93.1 |
| Montane grasslands & shrublands | 4.5 | 7.6 | 1.2 | 51.4 | 75.5 | 3.9 | 4.1 | 136.6 | 173.9 |
| Mediterranean forests, woodlands & scrub | 1.9 | 2.7 | 0.4 | 50.9 | 83.4 | 3.1 | 3.3 | 43.6 | 42.4 |
| Deserts & xeric shrublands | 25.8 | 28.5 | 4.4 | 53.3 | 76.4 | 2.9 | 3.0 | 48.0 | 49.7 |
| Tundra | 8.1 | 16.6 | 2.5 | 16.6 | 41.1 | 2.9 | 3.0 | 62.4 | 91.4 |
| Wetlands | 1.1 | 5.9 | 0.9 | 51.6 | 83.4 | 3.1 | 3.3 | 132.6 | 101.7 |
| Croplands | 24.0 | 63.2 | 9.7 | 52.3 | 80.7 | 2.1 | 2.2 | 65.5 | 66.5 |
| Global | 131.1 | 408.3 | 62.8 | 44.6 | 77.2 | 3.0 | 3.1 | 71.7 | 82.0 |

FC/BC: ratio of fungal necromass C to bacterial necromass C, FN/BN: ratio of fungal necromass N to bacterial necromass N, NecromassC/MBC: ratio of microbial necromass C to living microbial biomass C, NecromassN/MBN: ratio of microbial necromass N to living microbial biomass N.

**Extended Data Table 2 Soil stocks of amino sugars in topsoil (0-30 cm) and subsoil (30-100 cm) in different biomes.**

| Biomes | Area (million $km^{-2}$) | TAS (Gt) | | GluN (Gt) | | MurA | | Fungal C | | Bacterial C | | Fungal N | | Bacterial N | |
|---|---|---|---|---|---|---|---|---|---|---|---|---|---|---|---|
| | | 0-30 cm | 30-100 cm | 0-30 cm | 30-100 cm | 0-30 cm | 30-100 cm | 0-30 cm | 30-100 cm | 0-30 cm | 30-100 cm | 0-30 cm | 30-100 cm | 0-30 cm | 30-100 cm |
| Tropical & subtropical forests | 18.0 | 5.3 | 5.4 | 3.4 | 3.5 | 0.3 | 0.3 | 26.5 | 26.9 | 14.6 | 14.8 | 4.1 | 4.2 | 2.2 | 2.2 |
| Temperate forests | 10.6 | 4.7 | 5.1 | 3.1 | 3.4 | 0.1 | 0.1 | 26.4 | 28.5 | 5.6 | 6.1 | 4.1 | 4.4 | 0.8 | 0.9 |
| Boreal forests/Taiga | 14.8 | 10.6 | 16.4 | 7.0 | 10.9 | 0.3 | 0.5 | 58.7 | 91.1 | 14.9 | 23.2 | 9.1 | 14.2 | 2.2 | 3.4 |
| Tropical & subtropical grasslands, savannas & shrublands | 17.2 | 4.1 | 4.5 | 2.5 | 2.8 | 0.2 | 0.2 | 20.8 | 22.7 | 7.1 | 7.7 | 3.2 | 3.5 | 1.1 | 1.1 |
| Temperate grasslands, savannas & shrublands | 5.1 | 1.8 | 1.9 | 1.1 | 1.2 | 0.1 | 0.1 | 8.7 | 9.6 | 3.5 | 3.8 | 1.4 | 1.5 | 0.5 | 0.6 |
| Montane grasslands & shrublands | 4.5 | 1.2 | 1.1 | 0.8 | 0.7 | 0.04 | 0.03 | 6.6 | 6.0 | 1.7 | 1.6 | 1.0 | 0.9 | 0.3 | 0.2 |
| Mediterranean forests, woodlands & scrub | 1.9 | 0.4 | 0.4 | 0.3 | 0.3 | 0.02 | 0.01 | 2.2 | 2.1 | 0.7 | 0.7 | 0.3 | 0.3 | 0.1 | 0.1 |
| Deserts & xeric shrublands | 25.8 | 3.7 | 4.1 | 2.4 | 2.6 | 0.2 | 0.16 | 19.5 | 21.1 | 6.8 | 7.4 | 3.0 | 3.3 | 1.0 | 1.1 |
| Tundra | 8.1 | 2.0 | 2.8 | 1.1 | 1.5 | 0.1 | 0.09 | 8.8 | 12.3 | 3.1 | 4.3 | 1.4 | 1.9 | 0.5 | 0.6 |
| Wetlands | 1.1 | 0.6 | 0.9 | 0.4 | 0.5 | 0.02 | 0.03 | 2.9 | 4.4 | 1.0 | 1.4 | 0.5 | 0.7 | 0.1 | 0.2 |
| Croplands | 24.0 | 8.1 | 8.7 | 5.0 | 5.4 | 0.4 | 0.45 | 39.8 | 42.9 | 18.9 | 20.4 | 6.2 | 6.7 | 2.8 | 3.0 |
| Global | 131.1 | 46.0 | 58.7 | 29.3 | 37.5 | 1.8 | 2.21 | 240.5 | 308.8 | 80.1 | 99.5 | 37.4 | 48.0 | 11.9 | 14.8 |

TAS: Total amino sugar, GluN: glucosamine, MurA: muramic acid, FungalC: fungal necromass C, BacterialC: bacterial necromass C, FungalN: fungal necromass N, and BacterialN: bacterial necromass N.

# Supplementary Files

This is a list of supplementary files associated with this preprint. Click to download.

- SIGuide.docx
- SupplementaryData.xlsx